Experimental and Numerical Analysis of $S\text{-}CO_2$ Critical Flow for SFR Recovery System Design

Transactions of Korean Nuclear Society Spring Meeting, 2016

Min Seok Kim, Hwa-Young Jung, Yoonhan Ahn, Jekyoung Lee, Jeong Ik Lee

Ph.D. Candidate.
Dept. of Nuclear & Quantum Engineering, KAIST
minskim@kaist.ac.kr
+82-42-350-3882

NPNP

Introduction

Compact S-CO_2 Cycle Design

Turbomachinery Design

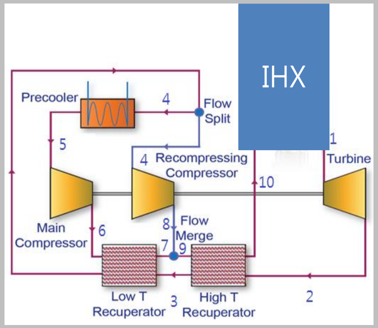

Single-Shaft Design (SSD)

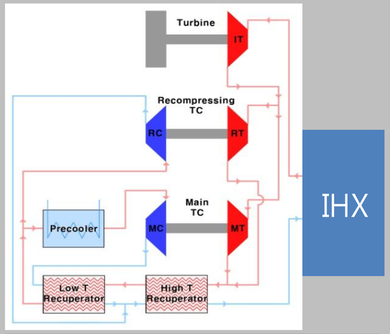

Triple-Shaft Design (TSD)

= 9 option

Module size

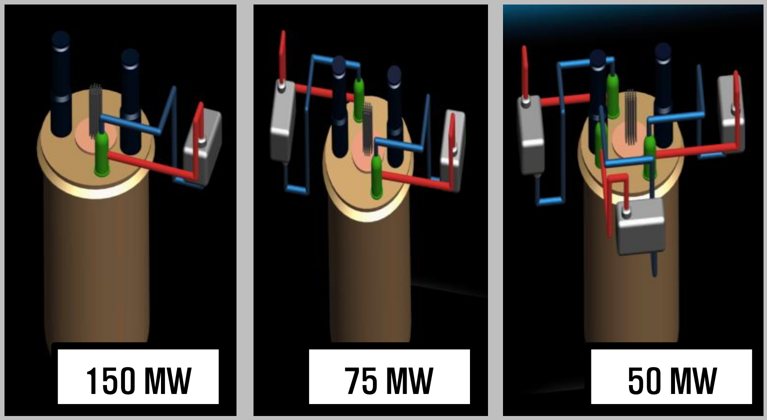

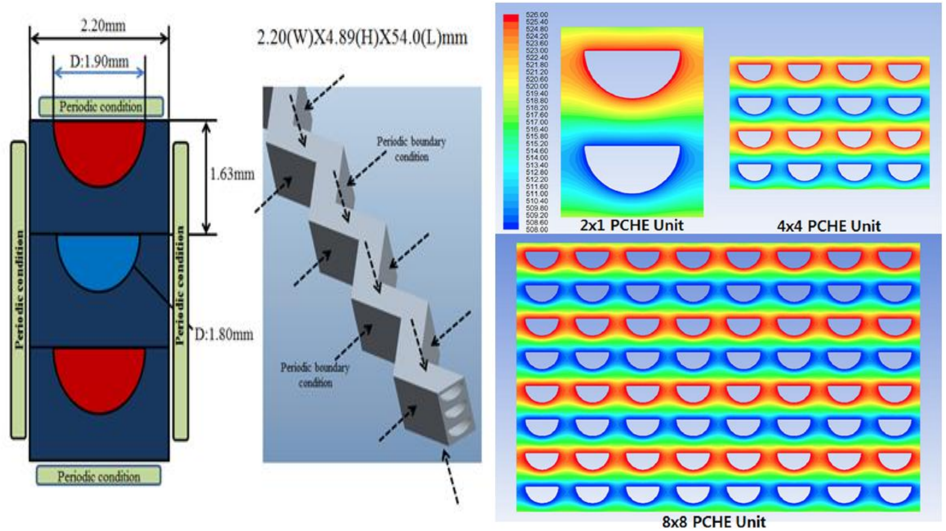

Variables		B (75 x 2)				
		IHX	HTR	LTR	PC	total
Effectiveness	%		95	95		
HS pressure drop	kPa	12.2	59.4	31.7	3.6	174.3
CS pressure drop	kPa	44.3	20.2	15.1	152.5	
Volume	m^3	1.2	7.8	17.7	2.2	28.9
Length	m	0.4	0.9	2	0.4	
Area	m^2	3.1	9.1	8.9	5.5	
CO_2 mass	kg	60.9	524.2	2136.6	229	2953 (5906)
Weight	ton	5.4	36.4	76.9	10.4	129.2
Pumping work	kW	47.3			606.6	31.6

Introduction

Research Objectives

- Motivation
  - To deal with the unavoidable leakage in rotating turbo-machinery
    - Since the S-CO_2 power cycle is a highly pressurized system, certain amount of leakage flow is inevitable in the rotating turbo-machinery via seals.
  - Need of a simple model for estimating the critical flow in a turbo-machinery seal
    - To predict the leakage flow rate and calculate the required total mass of working fluid in a S-CO_2 power system to minimize the parasitic loss.

- Goal of this study
  - CO_2 critical flow modeling
    - To identify the mass flow rate of CO_2 leakage in turbo-machinery
    - It is essential to design the CO_2 inventory recovery system.
  - CO_2 critical flow experiment
    - To verify the real CO_2 flow behavior and validate the CO_2 critical flow model with experimental results

Description of CO_2 Critical Flow Model

Preceding Studies on CO2 leak

- Sandia National Lab (SNL)
  - To lower windage loss, CO_2 in the rotor cavity was scavenged using a booster pump.

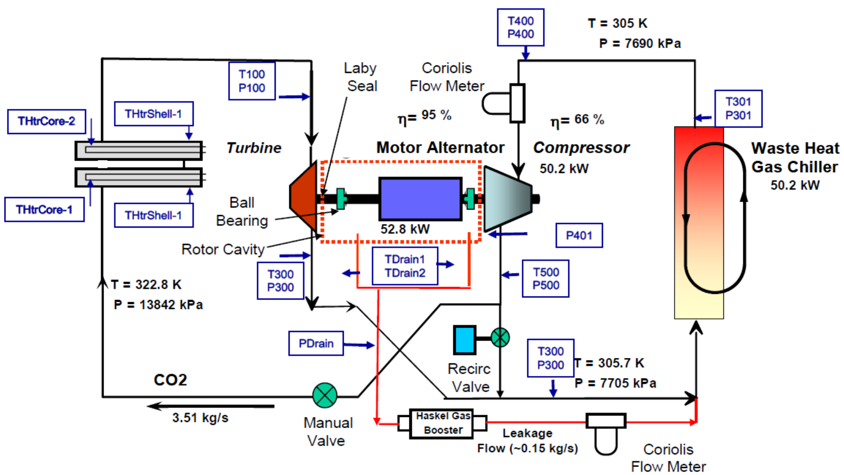

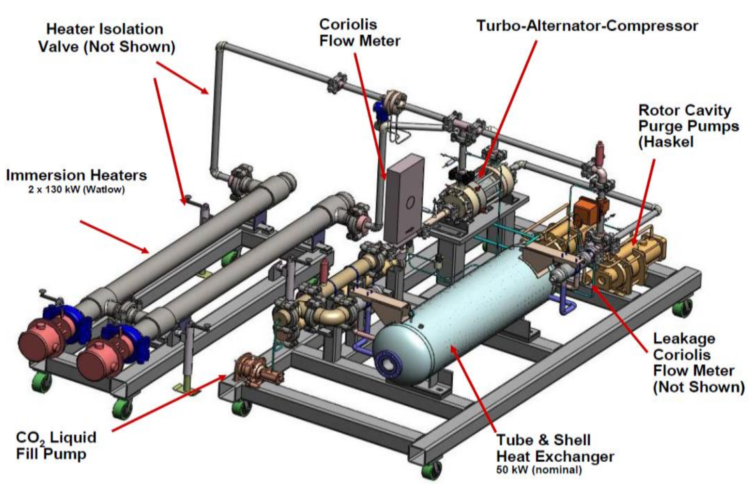

- Korea Atomic Energy Research Institute (KAERI)
  - To control the rotor cavity pressure, low-pressure tank, booster pump, and high-pressure tank were used.

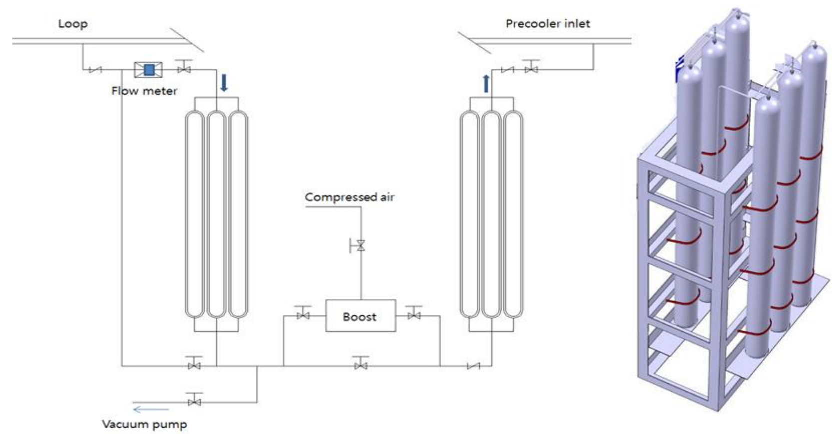

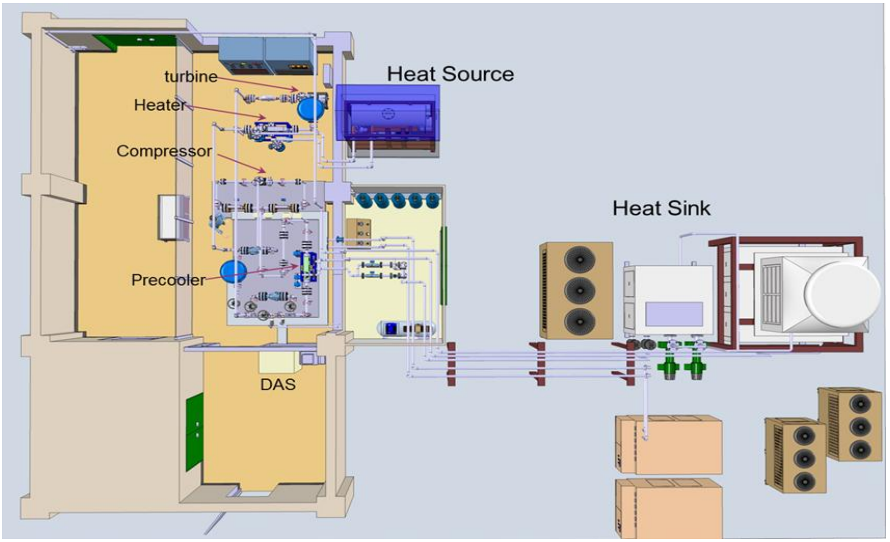

Description of CO_2 Critical Flow Model

Preceding Studies on CO_2 leak

- University of Wisconsin-Madison, 2009
  - To validate certain aspects of safety analyses
  - Data characterizing the behavior of supercritical fluids during a blowdown or rapid depressurization
  - Experiment to measure the critical mass flux for numerous stagnation thermodynamic conditions, geometry and outlet tube roughness.
  - 1D homogeneous equilibrium model was capable of relatively good (less than 10% error) prediction of the test data.
  - **It is not directly relative to critical flow in S-CO_2 turbo-machinery**

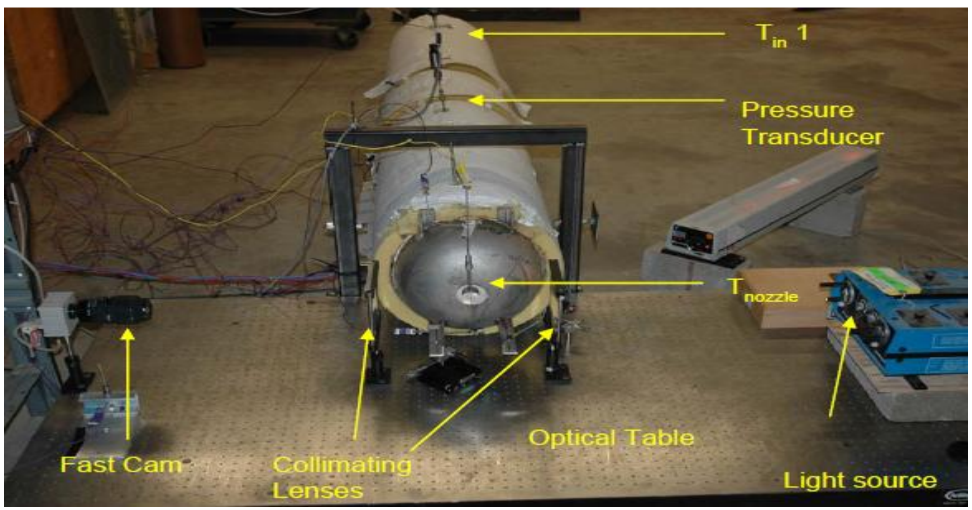

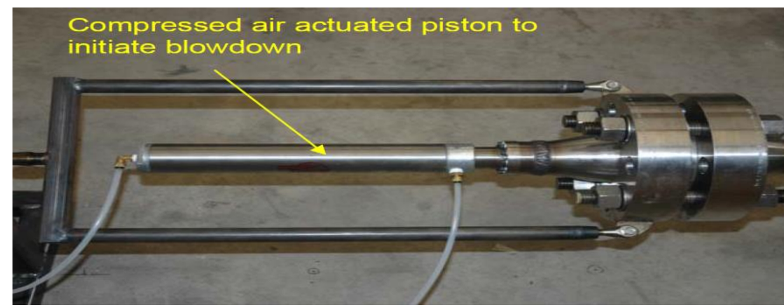

View of the opening systems

- Shadowgraphy set up using a fast fram camera to observe the shocks structure at the exit of the nozzles
- Some tests were conducted with a target plate located in front of the jet to measure the reaction force

Description of CO_2 Critical Flow Model

Preceding Studies on CO2 leak

- MAN Diesel & Turbo SE, 2015
  - An overview of numerical and experimental investigations on S-CO2 flow through carbon floating ring seals.
  - Simulation model considers the real gas effect, temperature deformation and the shaft rotation.
  - A comparison of the measured data to the model prediction shows an overall good agreement.
  - **It does not show the dynamic behavior of lower pressure stage.**

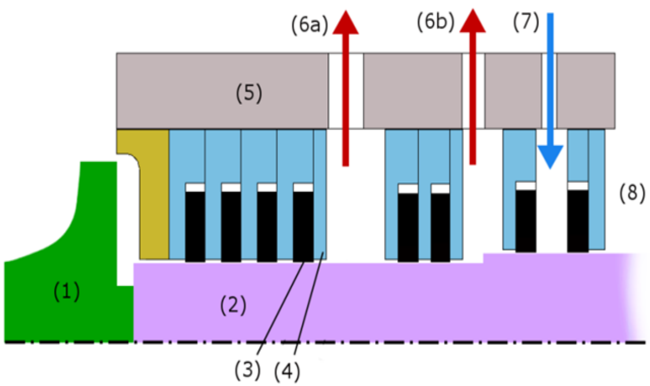

Design of a high pressure CRS system

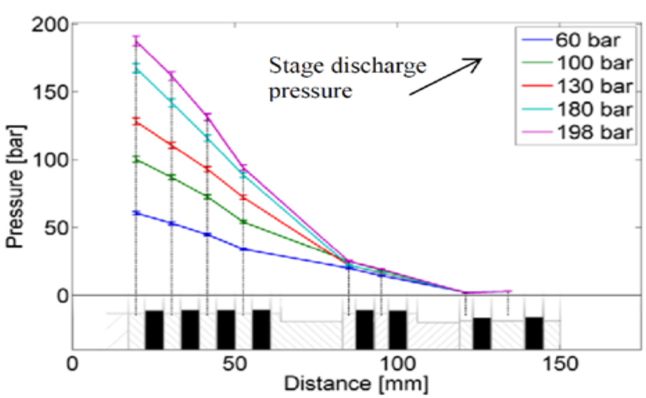

Measured pressure developments within the seal for relevant points

- Geometry and wall boundary conditions
  - $A = \pi(D+Y)Y,\ Y(x) = Y_0(x) + \Delta Y_s(x) - \Delta Y_R(x)$
- Kinematics
  - $u(x,y) = \begin{cases} \hat{u}(x)\cdot\left(2\frac{y}{Y}\right)^{\frac{1}{n_R}},\ 0 \le y \le \frac{Y}{2} \\ \hat{u}(x)\cdot\left(2(1-\frac{y}{Y})\right)^{\frac{1}{n_S}},\ \frac{Y}{2} \le y \le Y \end{cases},\ w(x,y) = \begin{cases} W-(W-\hat{w}(x))\cdot\left(2\frac{y}{Y}\right)^{\frac{1}{n_R}},\ 0 \le y \le \frac{Y}{2} \\ \hat{w}(x)\cdot\left(2(1-\frac{y}{Y})\right)^{\frac{1}{n_S}},\ \frac{Y}{2} \le y \le Y \end{cases}$
- Wall shear stress
  - $\tau_R = \frac{\lambda_R}{8}\rho\overline{c_R}^2,\ \tau_S = \frac{\lambda_S}{8}\rho\overline{c_S}^2,\ \tau_{R,ax} = \tau_R\frac{\hat{u}}{\widehat{c_{rel}}},$
    $\tau_{R,tan} = \tau_R\frac{\hat{w}_{rel}}{\hat{c}_{rel}},\ \tau_{S,ax} = \tau_S\frac{\hat{u}}{\hat{c}},\ \tau_{S,tan} = \tau_S\frac{\hat{w}}{\hat{c}}$
- Balance equations
  - $Q\left(\frac{\vartheta \boldsymbol{c}}{\vartheta t} + \boldsymbol{c}\cdot grad\boldsymbol{c}\right) = -grad\boldsymbol{p} + div\boldsymbol{T}$
- Heat transfer
  - $T_{shaft,wall} = T + \frac{q}{\alpha_{flow}}$

Description of CO_2 Critical Flow Model

Model Development

- Description of CO_2 critical flow model

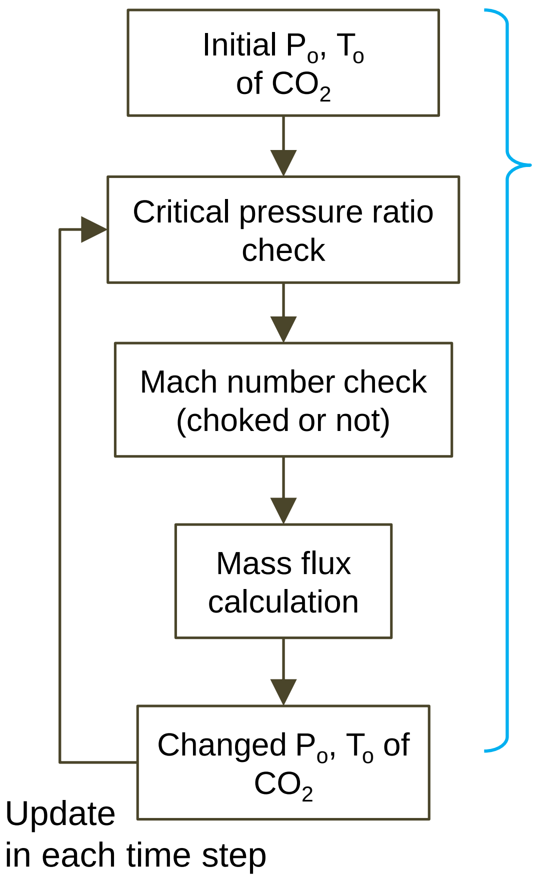

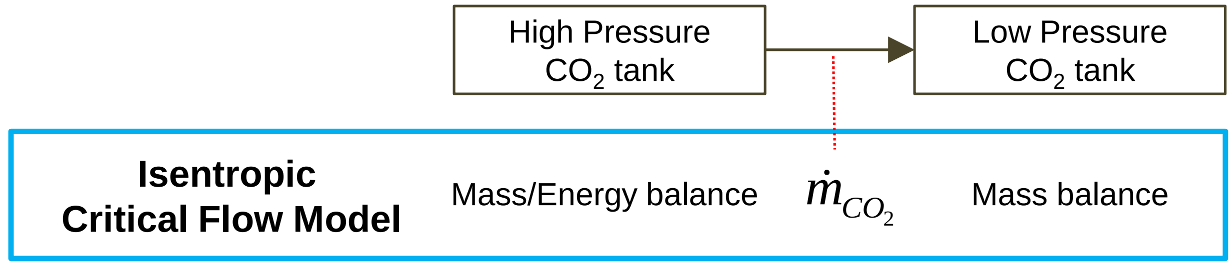

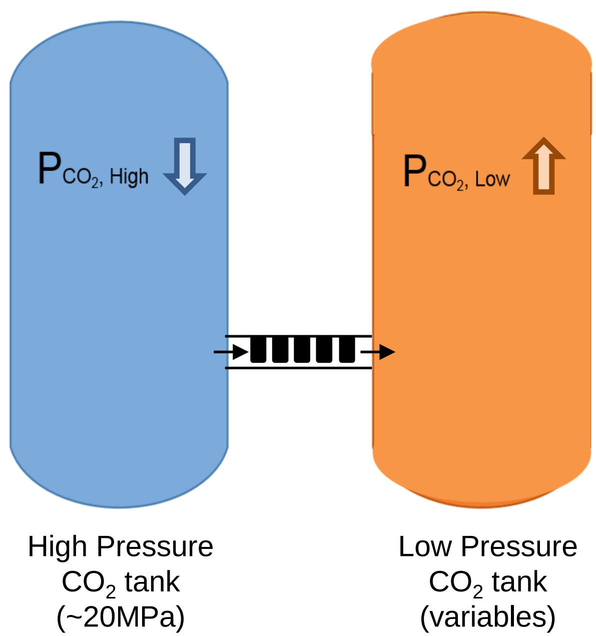

Fig. Mechanism of CO_2 leak in the simplified model for numerical analysis

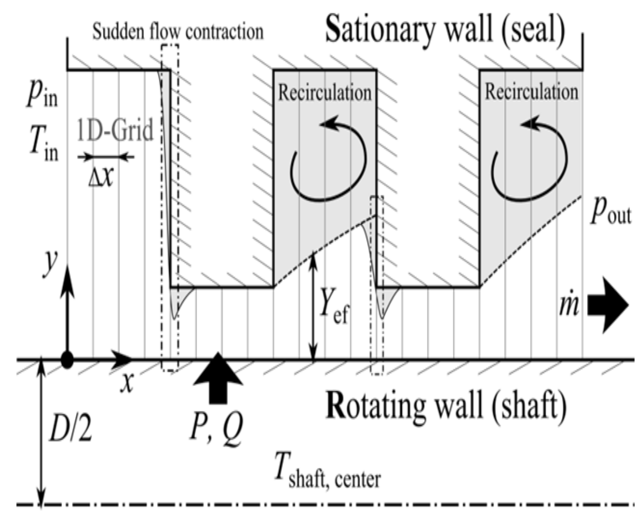

Fig. Mode sketch

Description of CO_2 Critical Flow Model

Model Development

- Assumptions for model

Isentropic critical flow model
• CO_2 in operating condition behaves like an ideal gas. (Compressibility factor ≈ 1) • CO_2 is stagnant in the CO_2 tanks. • Whether the flow is choked or not depends on the conditions of high pressure CO_2 tank and the back pressure. • Choking occurs at the nozzle exit. • The under-expansion of CO_2 at the nozzle exit is neglected.

- Used governing equations for model

Isentropic critical flow model

- $$\frac{P_{CO_2}}{P_{critical}} = \left(1 + \frac{\gamma - 1}{2}\right)^{\gamma/(\gamma-1)}$$
- $$M_{exit} = \sqrt{\frac{2}{\gamma - 1}\left[\left(\frac{P_{CO_2}}{P_{exit}}\right)^{(\gamma-1)/\gamma} - 1\right]}$$
- $$G = \frac{P_{CO_2}}{\sqrt{RT_{CO_2}}}\sqrt{\gamma}M_{exit}\left(1 + \frac{\gamma - 1}{2}M_{exit}^2\right)^{-\frac{\gamma+1}{2(\gamma-1)}}$$
- $$\dot{m} = \rho VA = GA$$

NPNP Nuclear Power & Propulsion Laboratory

CO_2 Critical Flow Experiment

Designed Experimental Facility

- Objectives
  - To **validate** the critical flow model with experimental results

- Description of experiment
  - Measuring pressure/temperature variation during the CO_2 injection
  - Calculating **CO_2 mass flux** with measured pressure/temperature at the nozzle exit

Table. Design specifications for experimental system

	Design Parameters	
High/Low-pressure tank	Pressure (MPa)	22
	Temperature (℃)	200
	Volume (L)	47 (I.D.: 200mm, H: 1,500mm)
Pipe connecting two tanks	I.D. (mm)	57
	Length (mm)	1090
Heater (Jacket-type)	Electric capacity (kW)	5
Valve type	Ball valve	

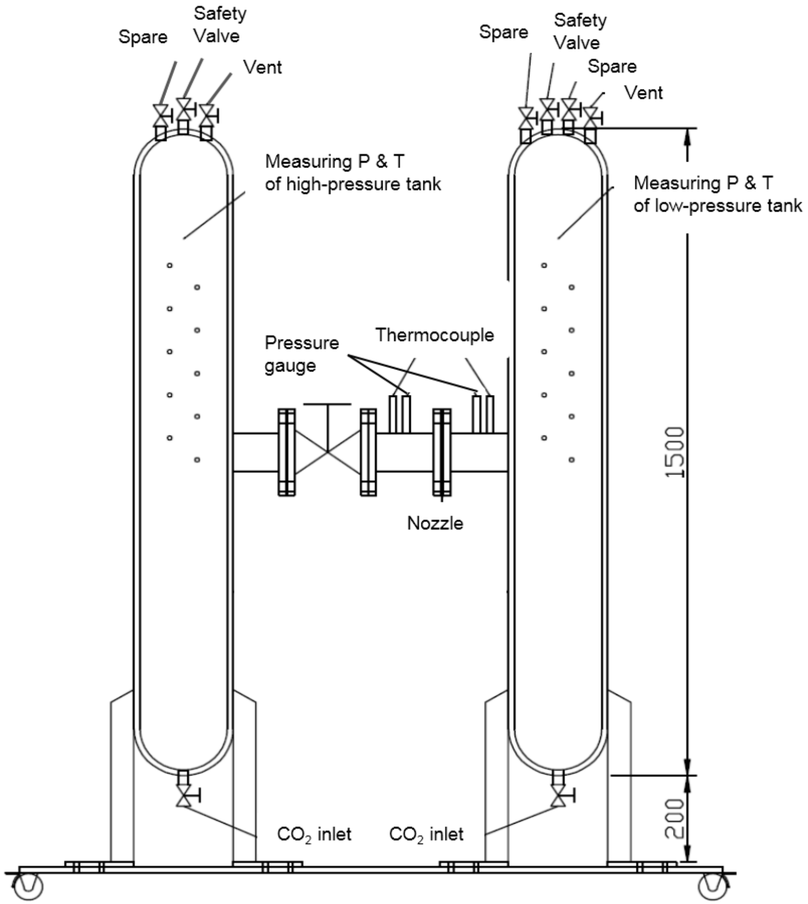

Fig. Conceptual design of experimental facility for CO_2 leak simulation

NPNP

CO_2 Critical Flow Experiment

Designed Experimental Facility

- Experiment procedure
  - **Close** the **ball valve** to separate the high and low pressure tanks
  - **Insert** the **nozzle** between high-pressure CO_2 tank and low-pressure CO_2 tank
  - **Fill** the high-pressure tank with **CO_2** from a storage tank until the pressure reaches the maximum pressure
  - **Control** the **initial temperature** of high-pressure CO_2 tank to meet the target point
    - Jacket type heater covered the external of high pressure tank
  - **Set** the **target initial conditions** by controlling the heater and the vent valve
  - **Turn off** the **heater** and **open** the **ball valve** by hydraulic power of compressed air
  - **Measure all temperatures and pressures** in each point every time until the CO_2 reaches equilibrium

Fig. Experimental Facility for CO_2 leak simulation

Table. Experimental conditions

Parameters	Conditions	
Nozzle diameter (mm)	1.5	
Nozzle length (mm)	5.0	
Pressure (MPa)	High-pressure tank	10~20
	Low-pressure tank	0.101
Temperature (℃)	High-pressure tank	100~150
	Low-pressure tank	15

CO_2 Critical Flow Experiment

Experiment Results

- Result generating process for CO_2 critical flow model and experiment

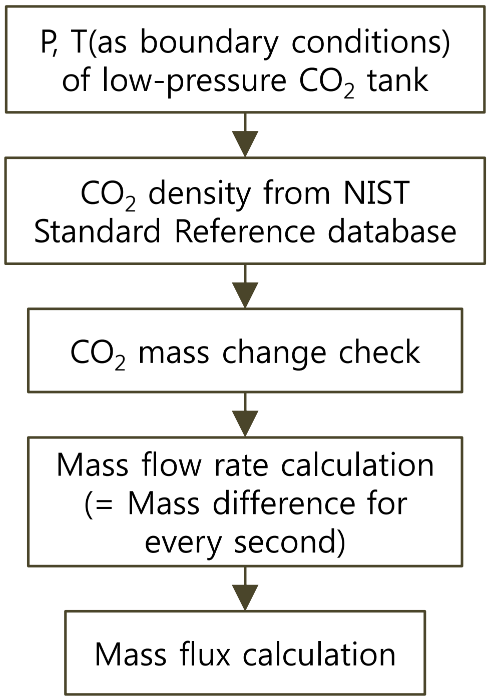

Figure. Flow diagram 1
(Experimental tank P, T)

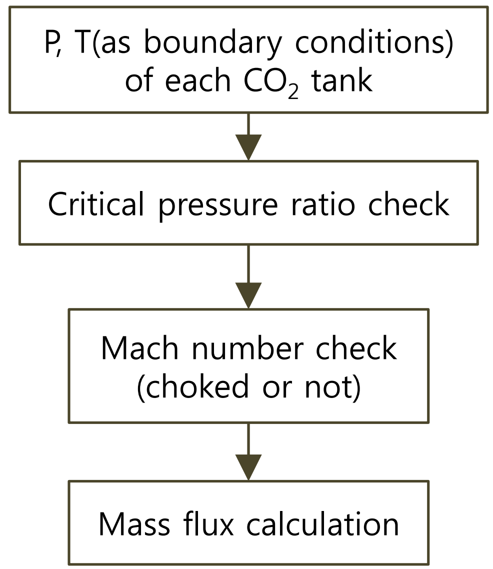

Figure. Flow diagram 2
(Exp. tank P,T + Code critical flow)

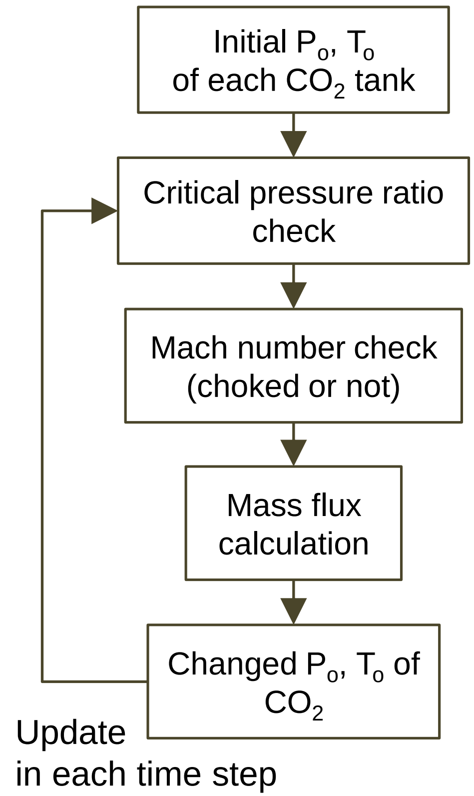

Figure. Flow diagram 3
(t=0: Exp. tank P,T + Code critical flow,
t>0: Code tank P,T + Code critical flow)

CO_2 Critical Flow Experiment

Experiment Results

- Comparison of all experiment results

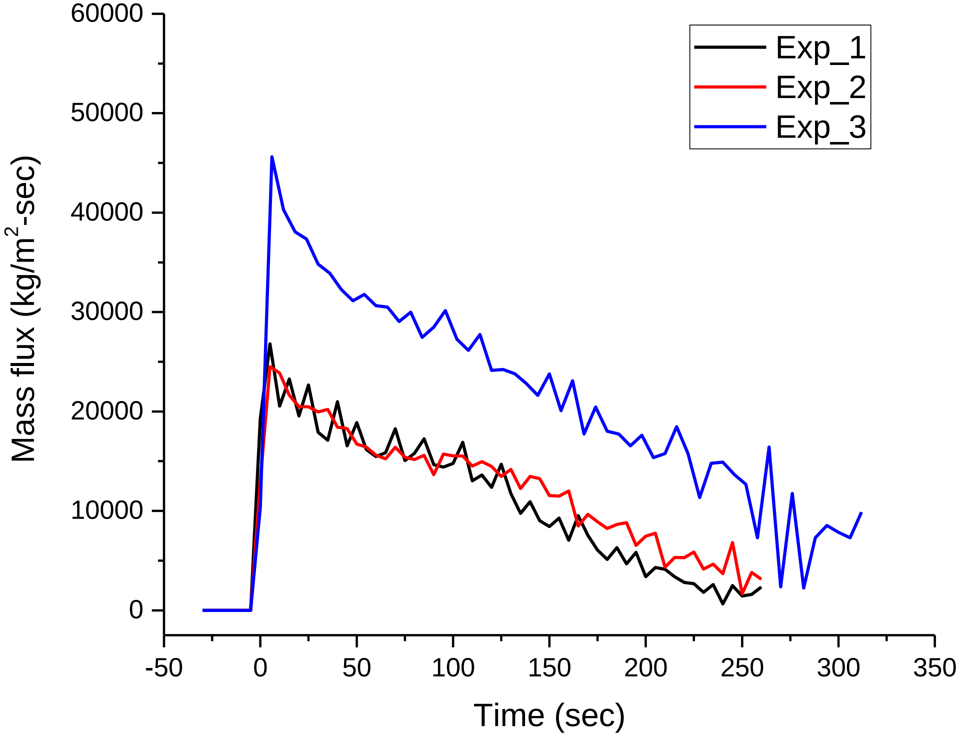

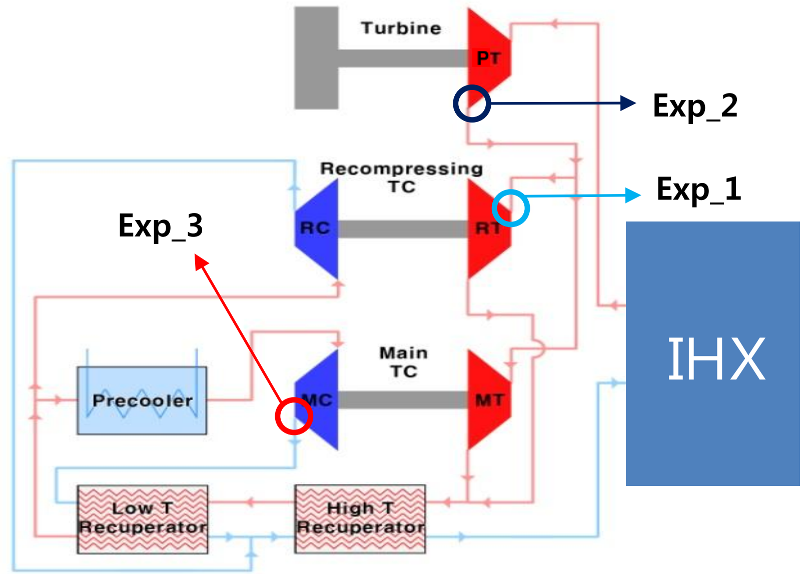

Fig. Triple-shaft design for S-CO_2 recompression cycle

Table. Experiment initial condition

		Exp_1	Exp_2	Exp_3
High-pressure tank	P (MPa)	10.01	13.43	20.16
	T (℃)	103.32	161.50	151.17
Low-pressure tank	P (MPa)	0.101	0.101	0.101
	T (℃)	14.50	15.60	14.10

CO_2 Critical Flow Experiment

Experiment Results

- Uncertainty analysis

$$G = \frac{1}{A_{nozzle}} \cdot \frac{\Delta m}{\Delta t} = f(A_{nozzle}, \Delta m, \Delta t)$$

$$\sigma_G{}^2 = (\frac{\vartheta f}{\vartheta \Delta m} \cdot \sigma_{\Delta m})^2 + (\frac{\vartheta f}{\vartheta \Delta t} \cdot \sigma_{\Delta t})^2 + (\frac{\vartheta f}{\vartheta A_{nozzle}} \cdot \sigma_{A_{nozzle}})^2$$

$$\sigma_V{}^2 = (\frac{\vartheta h}{\vartheta D_{tank}} \cdot \sigma_{D_{tank}})^2 + (\frac{\vartheta h}{\vartheta L} \cdot \sigma_L)^2$$

$$\sigma_\rho{}^2 = (\frac{\vartheta \rho(P,T)}{\vartheta P} \cdot \sigma_P)^2 + (\frac{\vartheta \rho(P,T)}{\vartheta T} \cdot \sigma_T)^2$$

$$\sigma_{\Delta m}{}^2 = (\frac{\vartheta g}{\vartheta V} \cdot \sigma_V)^2 + (\frac{\vartheta g}{\vartheta \rho_2} \cdot \sigma_{\rho_2})^2 + (\frac{\vartheta g}{\vartheta \rho_1} \cdot \sigma_{\rho_1})^2$$

$$\sigma_{A_{nozzle}}{}^2 = (\frac{\vartheta I}{\vartheta D_{nozzle}} \cdot \sigma_{D_{nozzle}})^2$$

$$\Delta m = V(\rho_2 - \rho_1) = V\{\rho(P_2, T_2) - \rho(P_1, T_1)\} = g(V, \rho_2, \rho_1)$$

$$V = \frac{\pi D_{tank}{}^2 L}{4} = h(D_{tank}, L) \qquad A_{nozzle} = \frac{\pi D_{nozzle}{}^2}{4} = I(D_{tank})$$

$$\begin{cases} D_{nozzle} = 1.5 \text{ mm} \\ \Delta t = 1\ sec \\ D_{tank} = 200\ mm \\ \sigma_T = \pm(0.15 + 0.002 \times T)\ ℃ \\ \sigma_P = \pm(0.025\%) \times P\ kPa \\ \sigma_{\Delta t} = \pm 0.03\ sec \\ \sigma_{D_{nozzle}} = \pm 0.02\ mm \\ \sigma_{D_{tank}} = \pm 0.5\ mm \\ \sigma_L = \pm 1.2\ mm \end{cases}$$

NPNP

CO_2 Critical Flow Experiment

Experiment Results

- Comparison of 1st experiment and modeling result

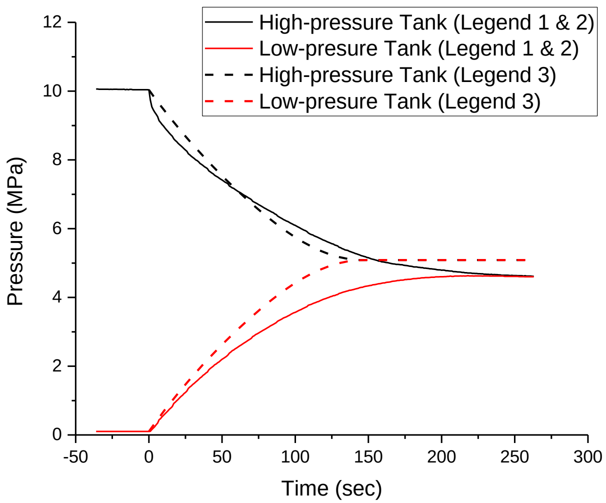

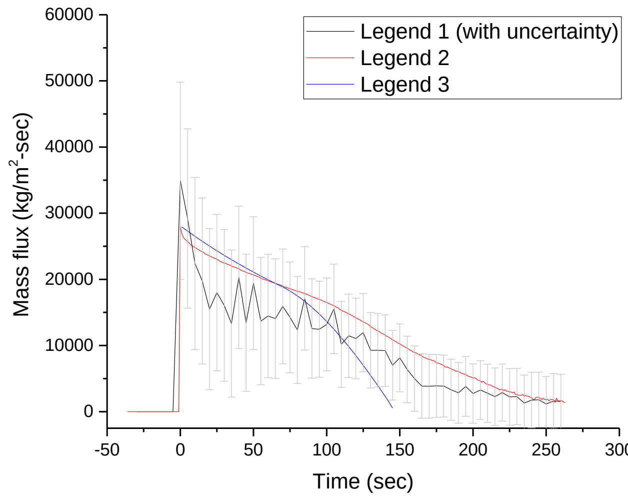

Fig. Mass flux result of experiment and model (Using high-pressure tank)

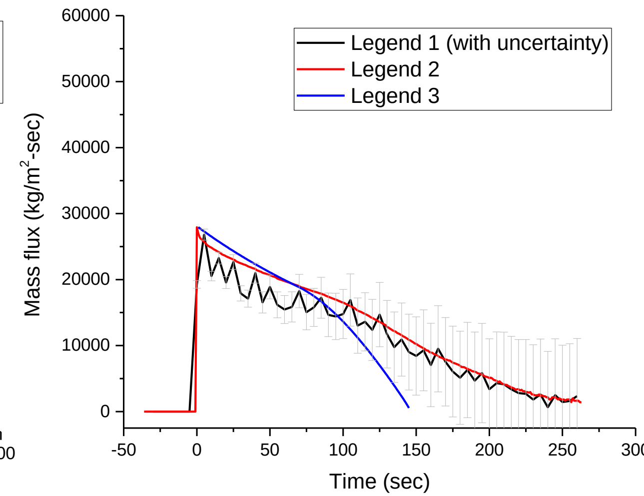

Fig. Mass flux result of experiment and model (Using low-pressure tank)

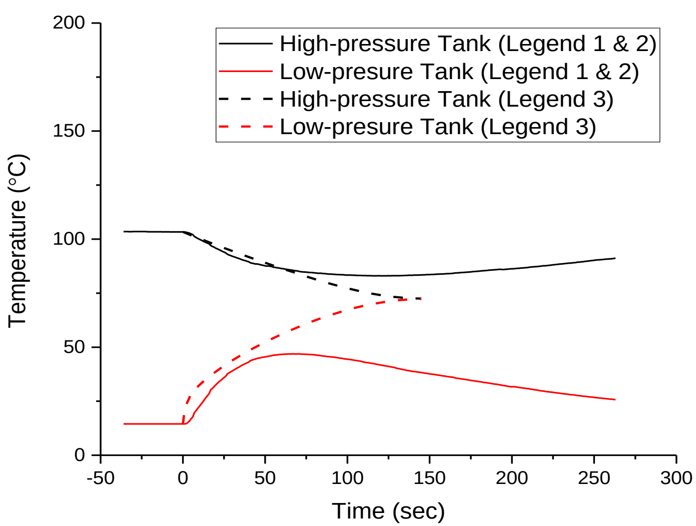

Table. Experiment initial condition (Case 1)

	P (MPa)	T (℃)
High-pressure tank	10.04	103.3
Low-pressure tank	0.101	14.5

- Legend 1: Exp. Tank P,T
- Legend 2: Exp. Tank P,T + Code Critical Flow
- Legend 3: Exp. Tank Initial P,T + Code Tank P,T + Code Critical Flow

CO_2 Critical Flow Experiment

Experiment Results

- Comparison of 2nd experiment and modeling result

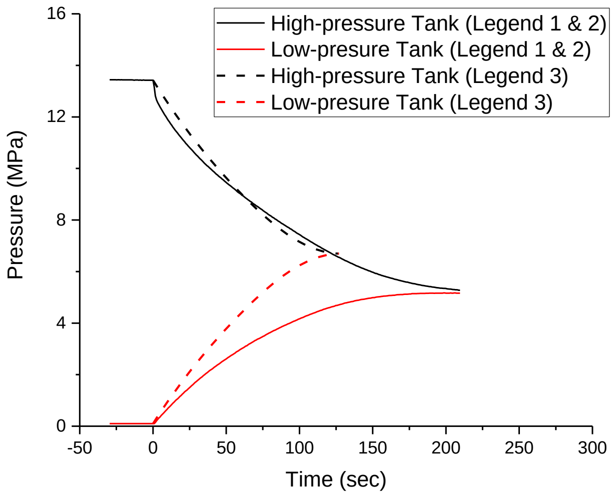

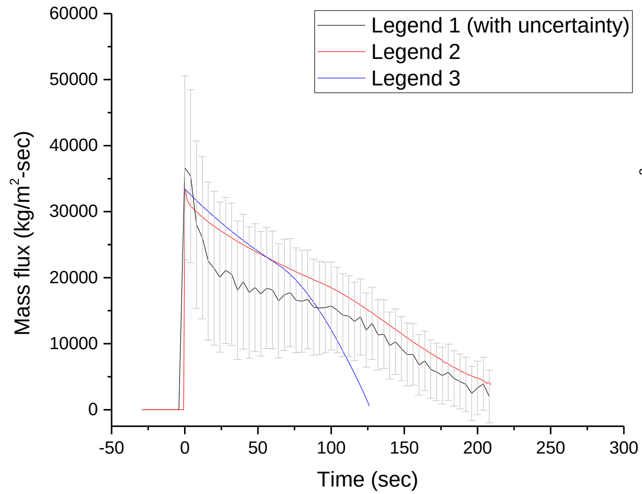

Fig. Mass flux result of experiment and model (Using high-pressure tank)

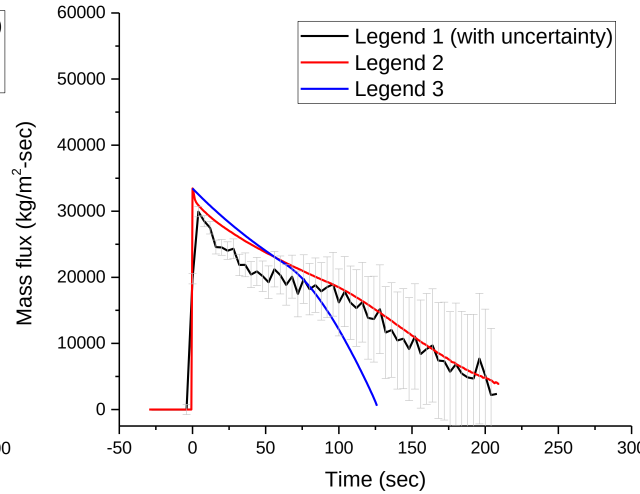

Fig. Mass flux result of experiment and model (Using low-pressure tank)

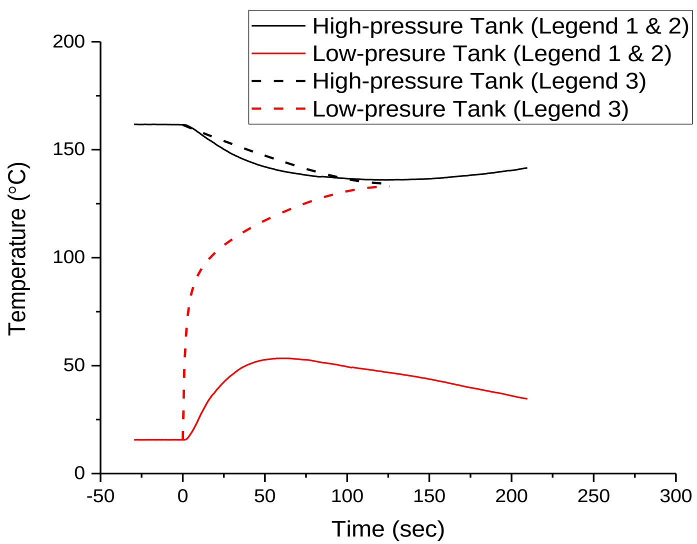

Table. Experiment initial condition (Case 2)

	P (MPa)	T (℃)
High-pressure tank	13.43	161.5
Low-pressure tank	0.101	15.6

- Legend 1: Exp. Tank P,T
- Legend 2: Exp. Tank P,T + Code Critical Flow
- Legend 3: Exp. Tank Initial P,T + Code Tank P,T + Code Critical Flow

CO_2 Critical Flow Experiment

Experiment Results

- Comparison of 3rd experiment and modeling result

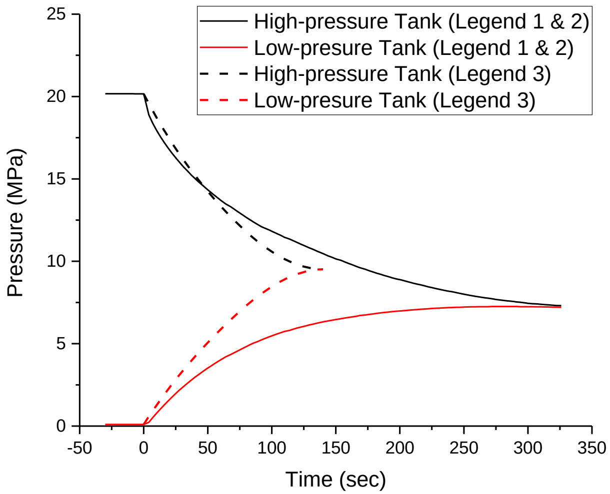

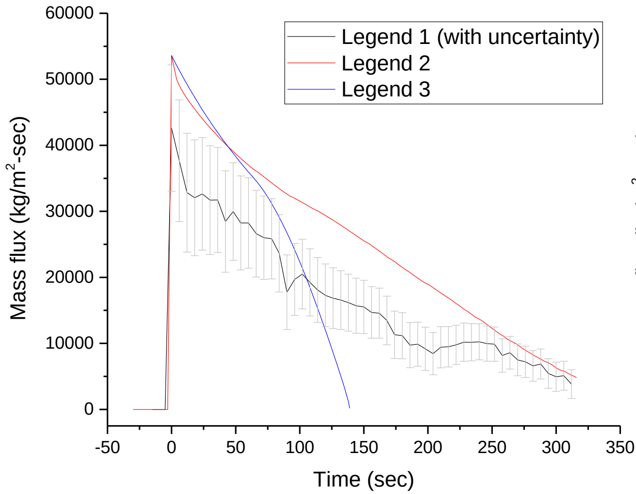

Fig. Mass flux result of experiment and model (Using high-pressure tank)

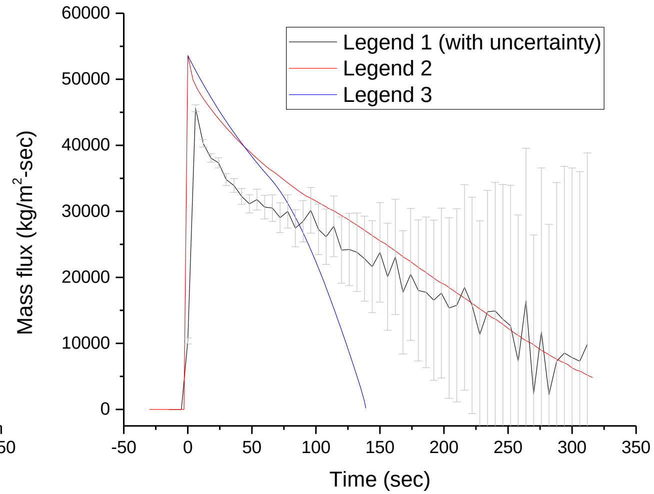

Fig. Mass flux result of experiment and model (Using low-pressure tank)

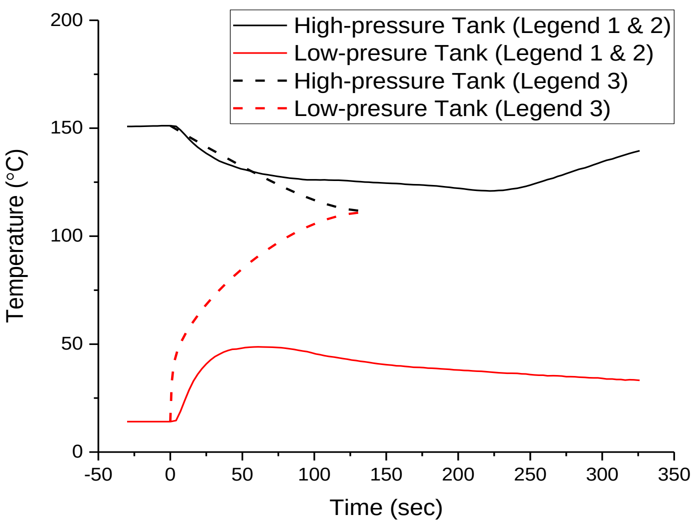

Table. Experiment initial condition (Case 3)

	P (MPa)	T (℃)
High-pressure tank	20.16	151.2
Low-pressure tank	0.101	14.1

- Legend 1: Exp. Tank P,T
- Legend 2: Exp. Tank P,T + Code Critical Flow
- Legend 3: Exp. Tank Initial P,T + Code Tank P,T + Code Critical Flow

CO_2 Critical Flow Experiment

Experiment Results

- Comparison of experiments and modeling result

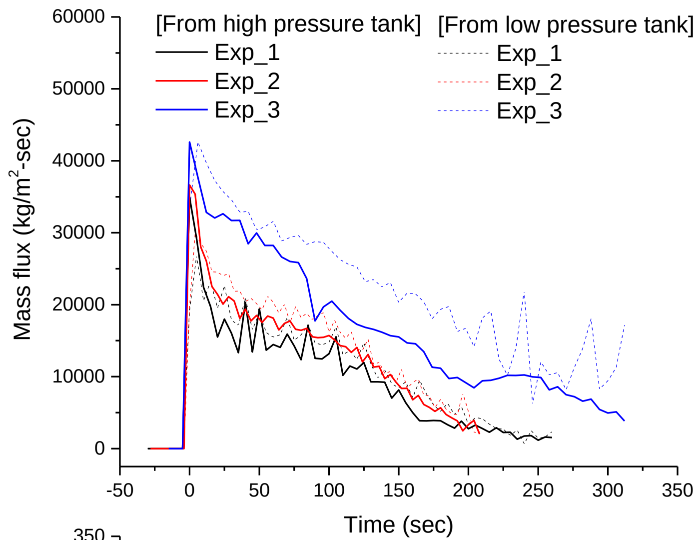

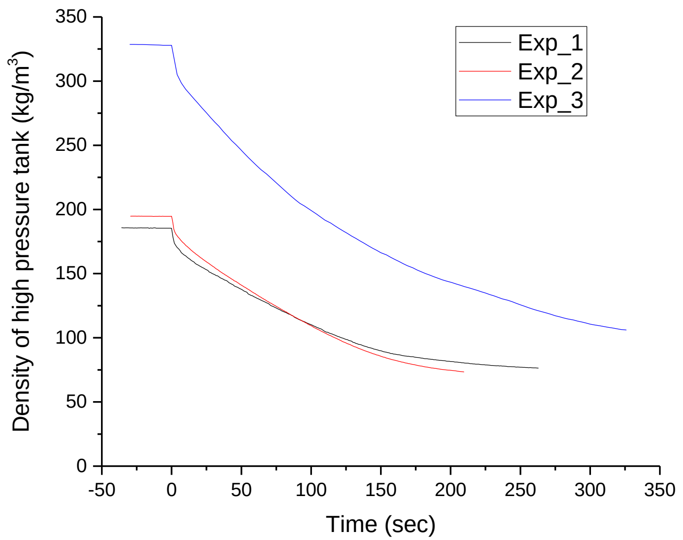

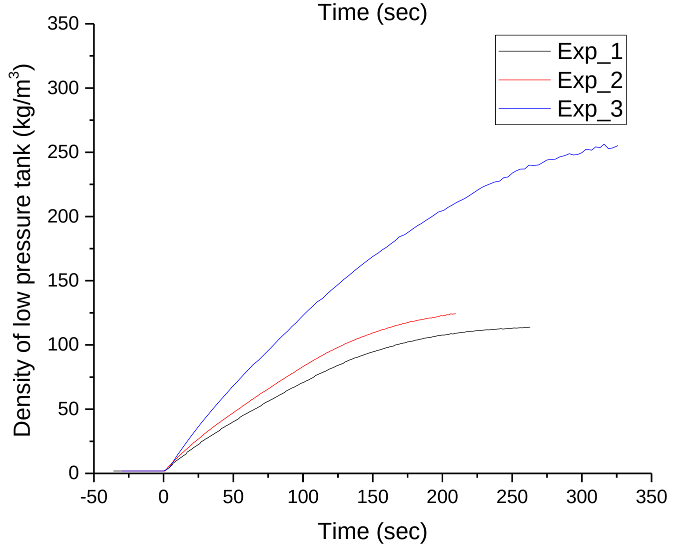

Table. Initial properties of all cases

	T (°C)	P (kPa)	ρ (kg/m^3)	h (kJ/kg)	s (kJ/kg-K)
Case 1	103.30	10.04	185.45	508.79	1.9420
Case 2	161.50	13.43	194.77	570.35	2.0500
Case 3	151.17	20.16	327.84	524.41	1.8814

CO_2 Critical Flow Experiment

Experiment Results

- Discussion on comparison with CO_2 critical flow model
  - The **mass flux** calculated by using the measured values has **similar trend** with the result of CO_2 critical flow model in all cases.
  - Although initial conditions of **exp.1 and 2** are different, **experiment results** are **similar.**
    - Because **density** dominates the **mass flux** and the densities of high and low-pressure tanks in exp. 1 and 2 have **similar trend**, **difference** of experiment results is very **small**.
  - **Uncertainty** of mass flux in high-pressure tank conditions **has contrast tendency** with in low-pressure tank.
    - Uncertainty σ_ρ is increased as density is increased and it increases uncertainty $\sigma_{\Delta m}$.
    - Consequently, Uncertainty σ_G is proportional to density since $(\frac{\vartheta f}{\vartheta \Delta m} \cdot \sigma_{\Delta m})^2$ term is dominant in σ_G.
  - **Uncertainty** of mass flux in low-pressure tank **is increased** around the equilibrium point.
    - **Equilibrium point** of low-pressure tank **is around** the **CO_2 critical point**.
    - $\frac{\vartheta \rho(P,T)}{\vartheta P}$, $\frac{\vartheta \rho(P,T)}{\vartheta T}$ around the CO_2 critical point have about 12 times value of normal condition and it causes the big uncertainty.
  - **Experimental temperature** trend is **somewhat different** with numerical temperature trend.
    - This difference seems to be due to **insufficient insulation** and **thermal inertia** of the CO_2 critical flow facility.
    - **Heat loss** from experimental facility seems to be **significant** since **only high-pressure tank was insulated**.
    - Second reason is the **thermal inertia** of the heater which surrounds the high-pressure tank and the tank itself.
    - The CO_2 critical flow model does **not consider heat transfer** to CO_2 from the tank wall and tanks have thermal inertia.

CO_2 Critical Flow Experiment

Experiment Results

- T-s and H-s diagram of each tank

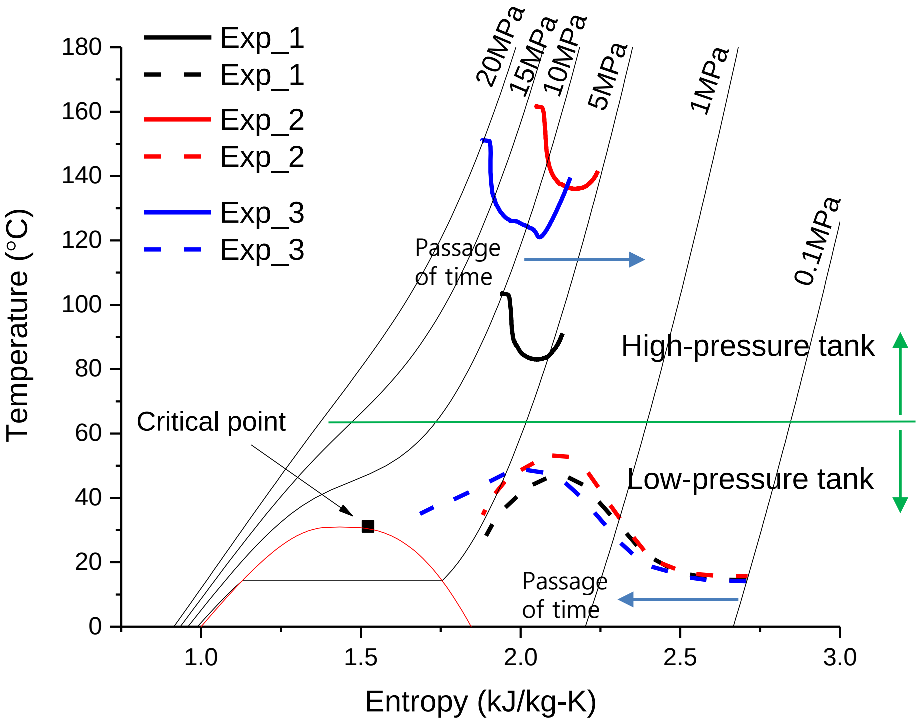

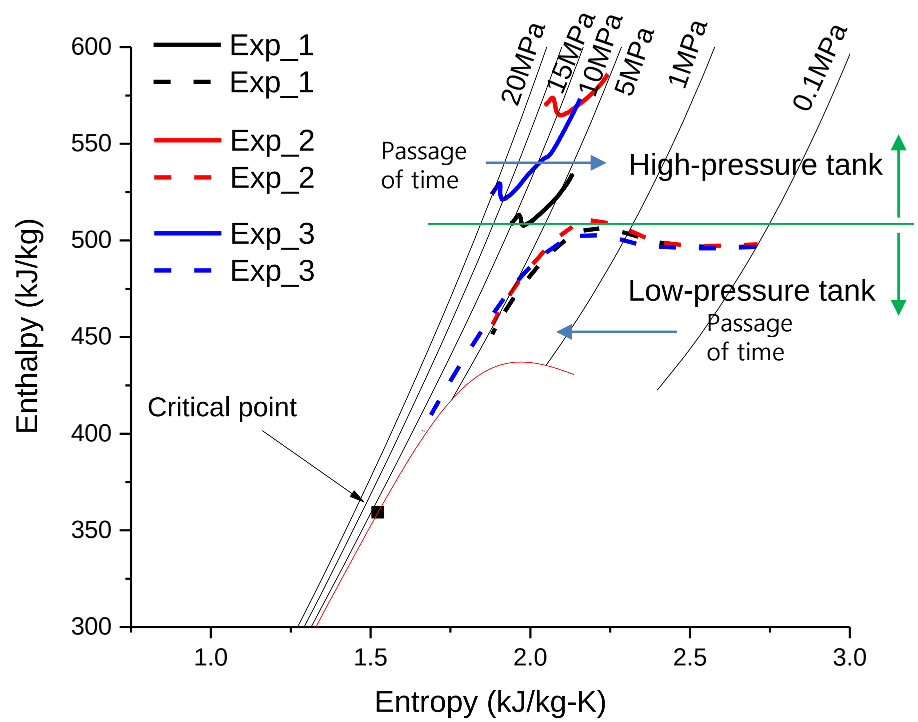

		Exp. 1	Exp. 2	Exp. 3
High-pressure tank	P (MPa)	10.04	13.43	20.16
	T (℃)	103.3	161.5	151.2
Low-pressure tank	P (MPa)	0.101	0.101	0.101
	T (℃)	14.5	15.6	14.1

CO_2 Critical Flow Experiment

Experiment Results

- Experiment with labyrinth seal geometry nozzle

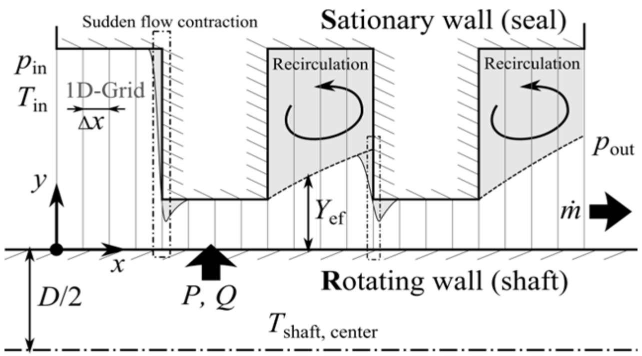

Figure. Labyrinth seal geometry

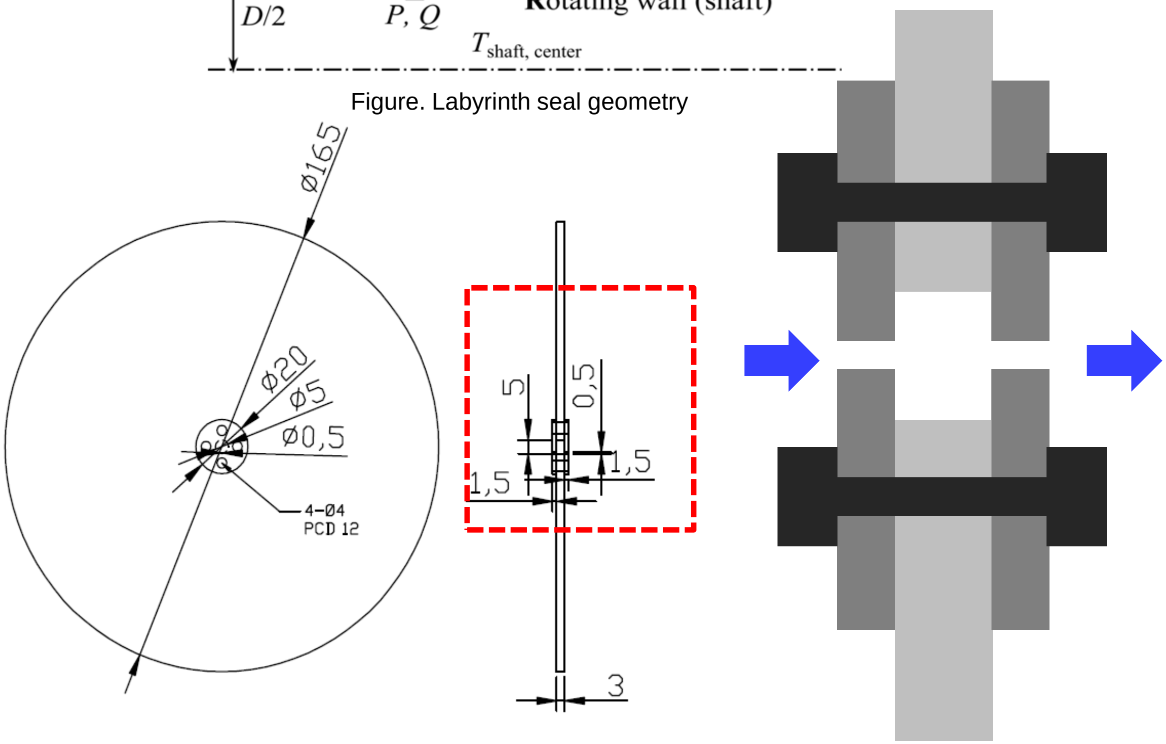

Figure. Conceptual design of real labyrinth seal geometry nozzle

NPNP

CO_2 Critical Flow Experiment

Experiment Results

- Comparison of results with simple nozzle and labyrinth seal geometry nozzle

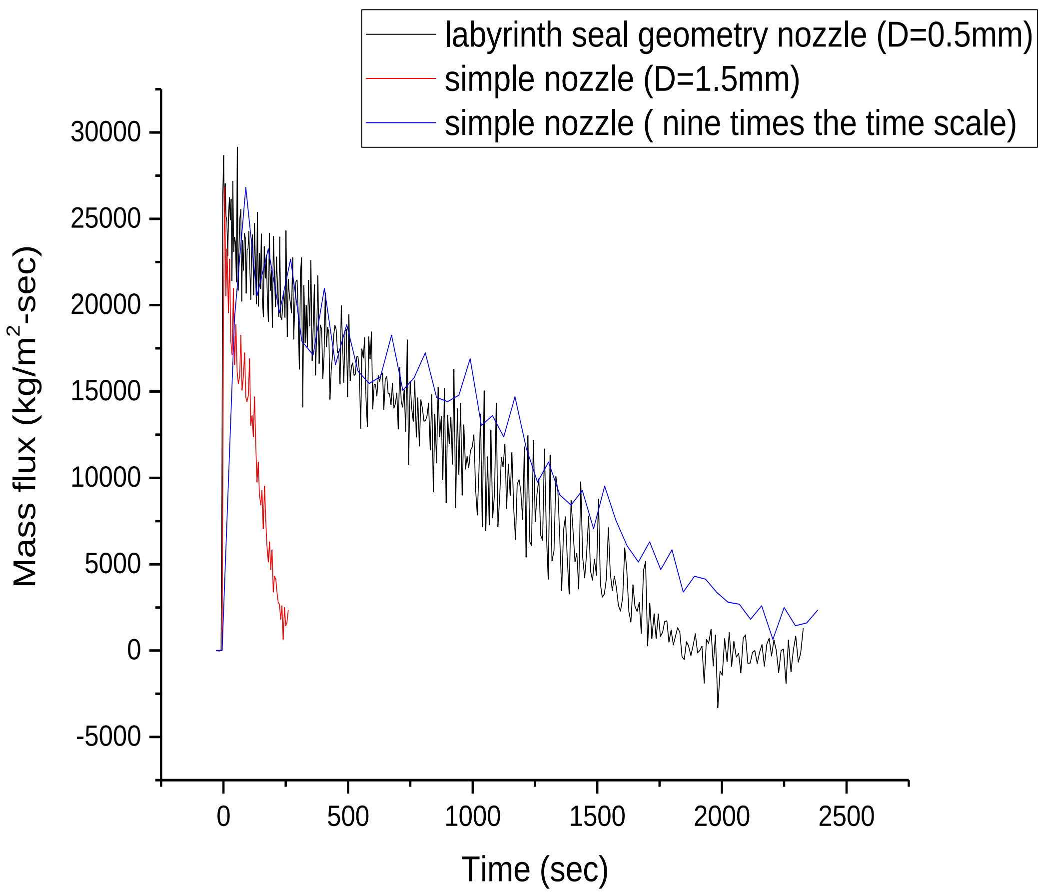

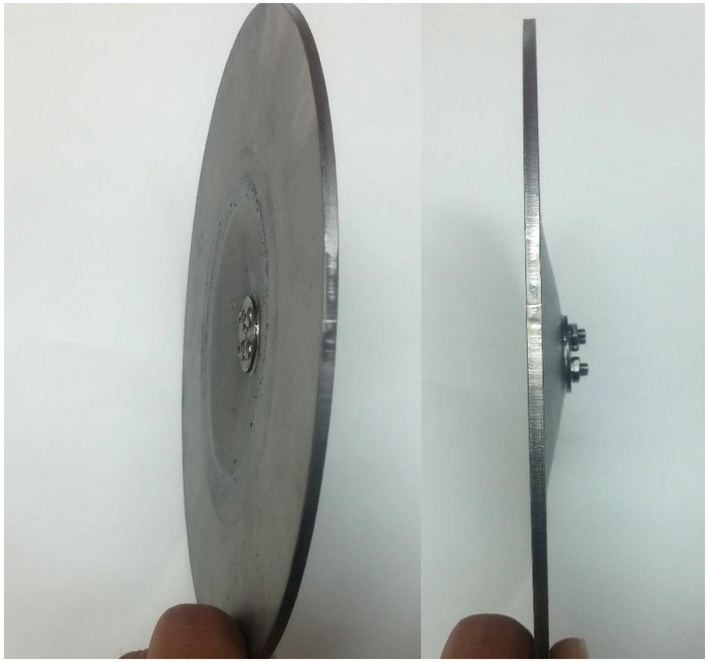

Table. Experiment initial condition (Case 1)

	P (MPa)	T (℃)
High-pressure tank	10.04	103.3
Low-pressure tank	0.101	14.5

Summary

Summary

- A simple model for estimating the CO_2 critical flow in a turbo-machinery seal was developed.
  - To identify the **mass flow rate** of CO_2 leakage in turbo-machinery to **minimize** the parasitic loss.

- Experiment of CO_2 critical flow was performed.
  - The **mass flux** calculated by using the measured values has **similar trend** with the result of CO_2 critical flow model in all cases.
  - It is identified that **developed isentropic critical flow model** can estimate **the behavior of CO_2 critical flow** in S-CO_2 turbo-machinery.

- Additional experiment with labyrinth seal geometry nozzle was performed.
  - The maximum **mass fluxes** of experiments with simple and labyrinth seal geometry nozzle are **almost the same** despite the different diameter.
  - **Labyrinth seal effect** is not identified due to **the lack of number of labyrinth seal** and **nozzle deformation**.

Further Works

Further works

- The **real gas effect, labyrinth seal geometry** and, **friction factor** will be considered in CO_2 critical flow model.

- **Insulation** in connecting pipes and low-pressure tank will be added and this will resolve the heat loss problem.

- **Experiment** of improved labyrinth seal geometry nozzle will be performed.

- Measurement of mass flow rate using **gyro sensor** will be considered to minimize the uncertainty of experiment results.

- Study of **CO_2 recovery system design** will be performed.
  - Seal configuration
  - Thermal efficiency loss with CO_2 leak rate and recovery point
  - Calculating the leak rate in turbo-machinery
  - Minimizing the parasitic loss by sensitivity analysis of CO_2 recovery process

Reference

Reference

- Hylla, E., Schildhauer, M., Bussow, R., Metz, K., Klawes, R., 2015, “Investigations on Transonic Flow of Super-critical CO_2 Through Carbon Ring Seals”. ASME Turbo Expo (2015).
- G.P. Mignot, M.H. Anderson, M.L. Corradini, Measurement of supercritical CO2 critical flow: effects of L/D and surface roughness, Nucl. Eng. Des. 239 (2009) 949–955.
- Hwa-Young Jung. Preliminary Safety Studies of Sodium-CO2 Heat Exchanger in SFR coupled with S-CO2 Brayton Cycle. Thesis, KAIST (2015).
- Stahley, J. S., Dry Gas Seal System Design Standards for Centrifugal Compressor Applications, Proceedings for the Thirty-first Turbomachinery Symposium, 2002
- Steven A. Wright, et al., 2010, Operation and Analysis of a Supercritical CO2 Brayton Cycle, SAND2010-0171
- Martin H.M.. Labyrinth Packings, Engineering, pp 35-36, 1908
- Robert Fuller, et al., 2012, Turbomahinery for Supercritical CO2 Power Cycles, Proceedings of ASME Turbo Expo 2012

THANK YOU